

# A Novel Computer-Aided Diagnostic System for Early Assessment of Hepatocellular Carcinoma

Ahmed Alksas<sup>1</sup>, Mohamed Shehata<sup>1</sup>, Gehad A. Saleh<sup>2</sup>, Ahmed Shaffie<sup>1</sup>, Ahmed Soliman<sup>1</sup>, Mohammed Ghazal<sup>3</sup>, Hadil Abu Khalifeh<sup>3</sup>, Ahmed Abdel Razek<sup>2</sup>, and Ayman El-Baz<sup>1</sup>

<sup>1</sup>BioImaging Lab, Bioengineering Department, University of Louisville, Louisville, KY, USA.

<sup>2</sup>Department of Radiology, Faculty of Medicine, University of Mansoura, Egypt.

<sup>3</sup>Faculty of Engineering, Abu Dhabi University, Abu Dhabi, UAE.

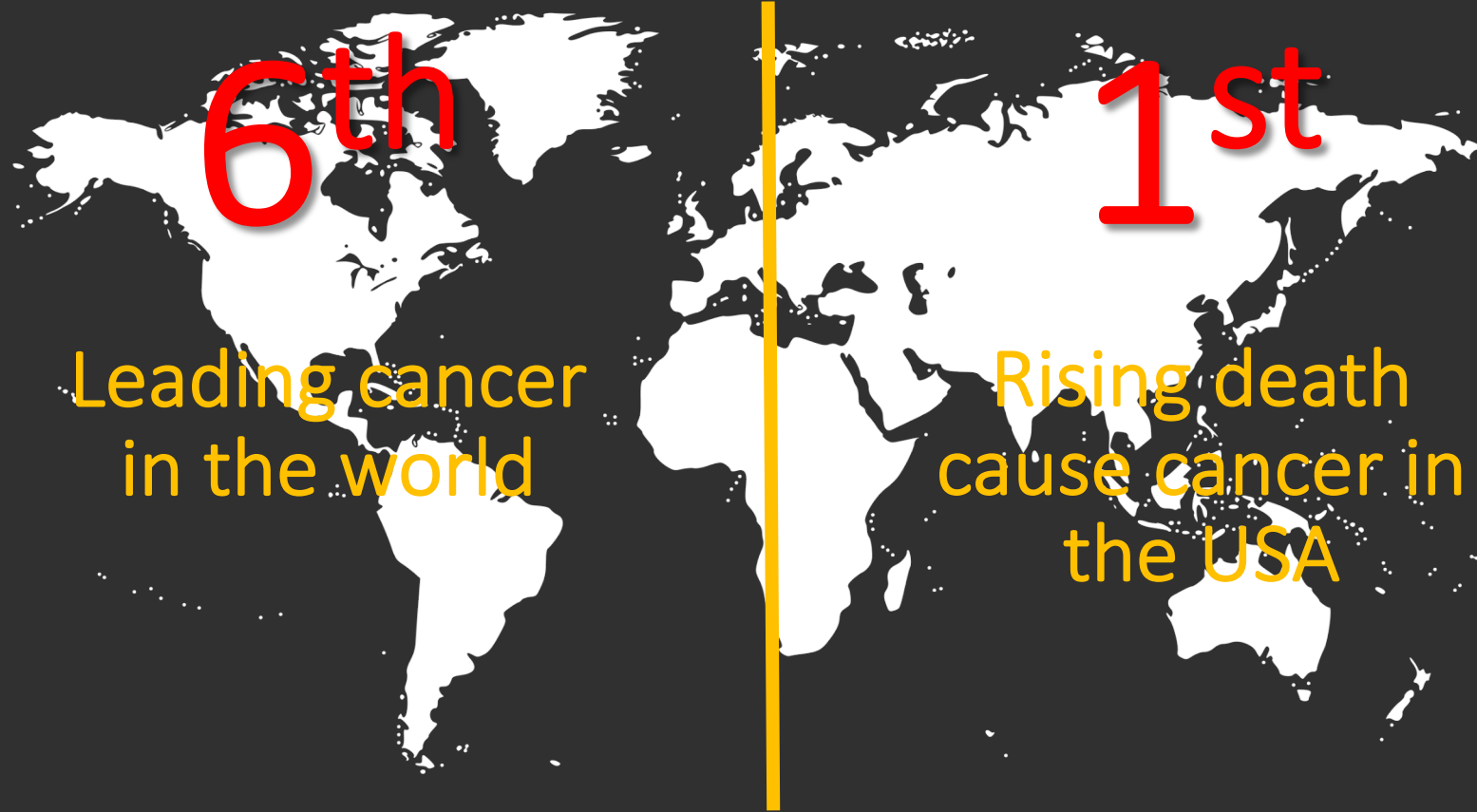


## Ahmed AlKsas, M.Sc.

Ph.D. Student @ CECS Department  
GRA @ BILAB, BE Department  
Speed School of Engineering,  
University of Louisville,  
Louisville, KY 40292  
Office: (502) 852-4032  
Email: [ammost01@louisville.edu](mailto:ammost01@louisville.edu)

ICPR 2020

# Research Motivations



# Research Motivations

Annual records:

- Worldwide : 800,000 new cases and 700,000 new deaths
- In the USA: 42,030 new cases and 31,780 deaths

At Global Averages:

1/5000 People

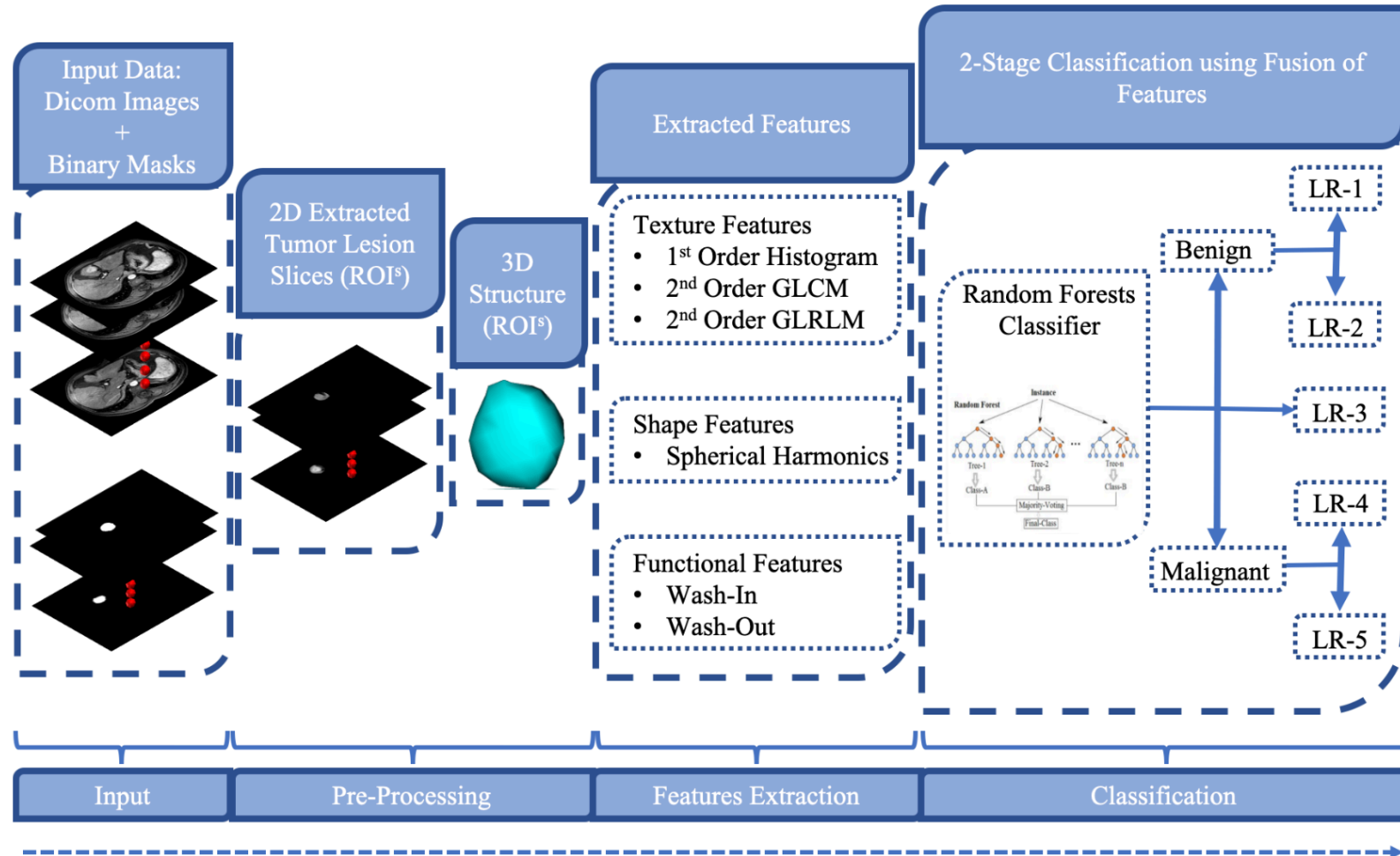
is in danger of contracting **HCC**

- HCC is a cancer arising from the liver cells.
- HCC is the most common primary liver disease, and its incidence is increasing.
- The prognosis of HCC is affected by its severity level when detected, as curative managements can be enough for early-stage HCC.
- Early assessment of liver cancer patients with HCC is of immense importance to provide the proper treatment plan.

# Current Diagnostic Tools & Limitations

- For **HCC**, a radiological diagnosis (**LI-RADS**) provides high diagnostic performance and is considered as the **Gold-Standard**, which makes the medical organizations depend only on highly-experienced radiologists for **HCC** diagnosis.
- Therefore, there is an urgent need for an **automated machine-learning based CAD system** to identify **HCC** and its grade to provide the proper treatment plan.

# Proposed Framework



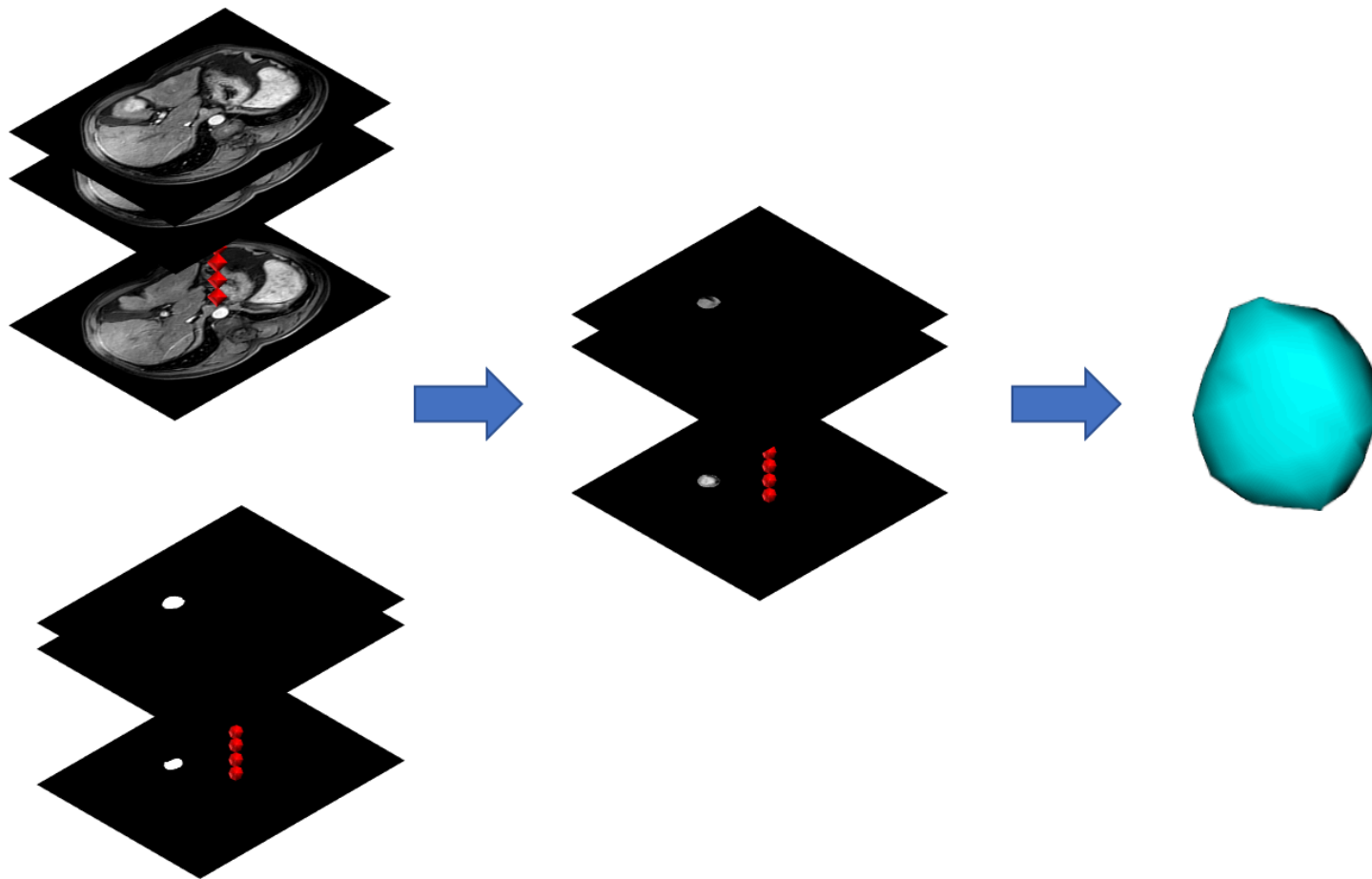
# Input: CE-MRI Data Collection

- ❑ A total of 85 patients with high risk of developing HCC without history of loco-regional treatment plan, (M = 61 and F = 24), provided their consent to participate in this study.
- ❑ They averaged an age of  $(55.131 \pm 7.12)$  ranging from 40 to 73 years old.
- ❑ 34 patients with benign tumors (LR-1 = 17 and LR-2 = 17), 17 with intermediate, and 34 with malignant tumors (LR-4 = 17 and LR-5 = 17)
- ❑ Acquisition parameters of MRI sequences are defined in the following Table:

Sequence	TR (msec.)	TE (msec.)	FOV (mm)	Matrix	Slice thickness (mm)	Slice gap (mm)	Flip angle
<b>T2</b>	$\geq 445$	26-28	230	160-144 $\times$ 240	6	3	NA
<b>T2 SPAIR</b>	2500-3000	80-100	230	144 $\times$ 144	6	3	NA
<b>Dynamic GRE (THRIVE)</b>	7.3	3.1	500	256 $\times$ 128	3	1	40

Acquisition parameters of MRI sequences. TR: repetition time; TE: echo time; FOV: field of view; SPAIR: spectral attenuated inversion recovery; GRE: gradient-recalled echo; THRIVE: T1-weighted, high-resolution isotropic volume examination.

# Liver Tumor Preprocessing



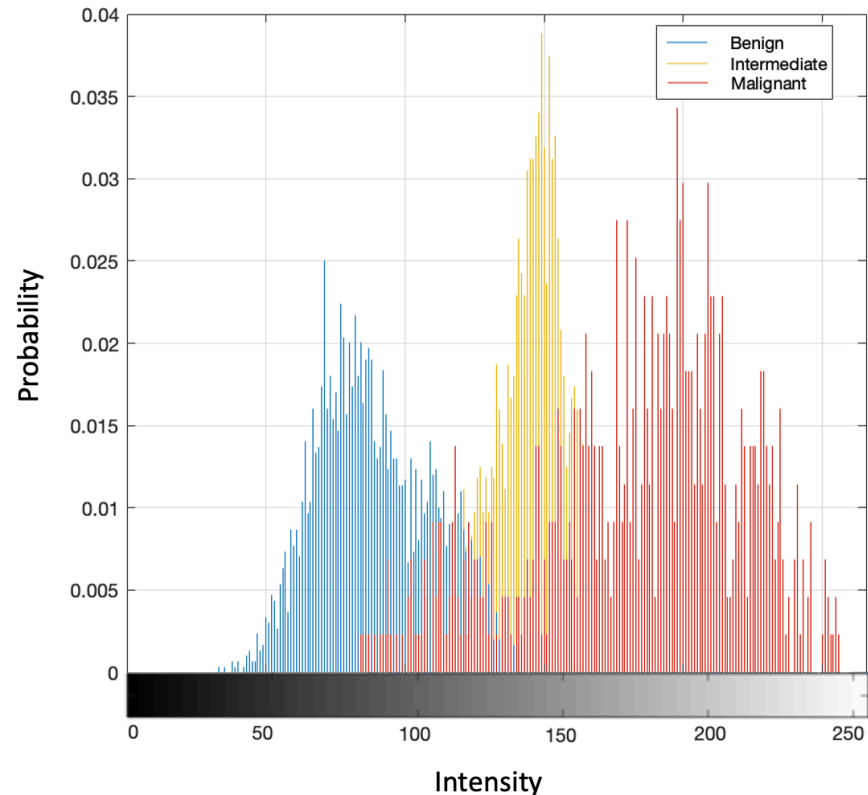


# Features Extraction: Texture Features

## 1<sup>st</sup> Order Texture Features

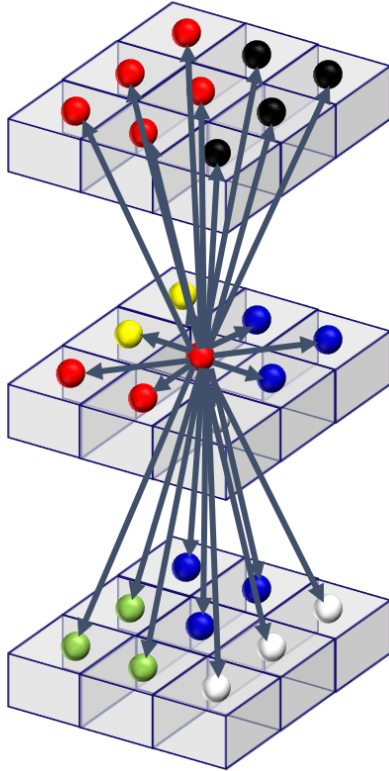
➤ Here, we extracted texture analysis features from the gray-level histogram of the four 3D constructed objects for each tumor lesion.

➤ The computed features are mean, variance, standard deviation, skewness, kurtosis, entropy, cumulative distribution function and gray-level percentiles.



# Features Extraction: Texture Features (cont'd)

A 3\*3\*3 Section from an HCC  
Tumor 3D object



Update



## 2nd Order GLCM

GLCM of the HCC  
Tumor 3D object

	+7+7	+4	+6	+3	+4	+2
	+4	+0	+0	+0	+0	+0
	+6	+0	+0	+0	+0	+0
	+3	+0	+0	+0	+0	+0
	+4	+0	+0	+0	+0	+0
	+2	+0	+0	+0	+0	+0

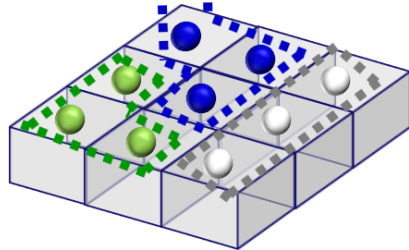
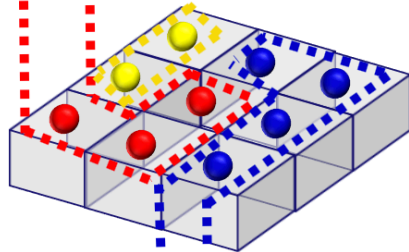
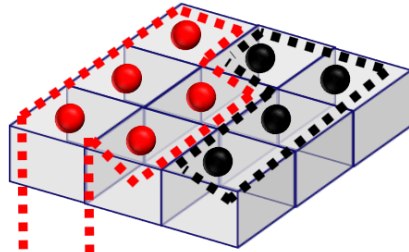
Represent different intensity levels

+value

The value to be added to the GLCM cells

# Features Extraction: Texture Features (cont'd)

A 3\*3\*3 Section from an HCC  
Tumor 3D object

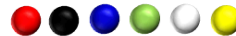


## 2nd Order GLRLM

GLRLM of the HCC  
Tumor 3D object

	1	2	3	4	5	6	7	8
Red	+0	+0	+0	+0	+0	+0	+0	+1
Black	+0	+0	+0	+1	+0	+0	+0	+0
Blue	+0	+0	+0	+0	+0	+0	+1	+0
Green	+0	+0	+1	+0	+0	+0	+0	+0
White	+0	+0	+1	+0	+0	+0	+0	+0
Yellow	+0	+1	+0	+0	+0	+0	+0	+0

Update



Represent different intensity levels

1 2 3 4 5 6 7 8

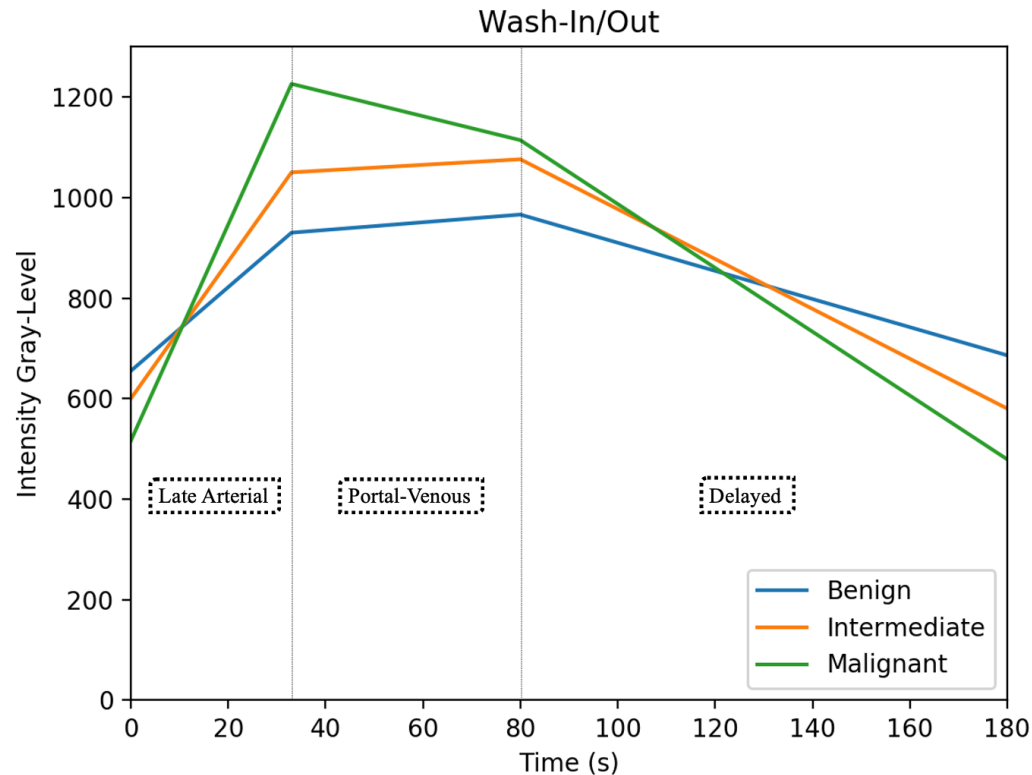
Represent different Run Lengths

+value

The value to be added to the GLRLM cells

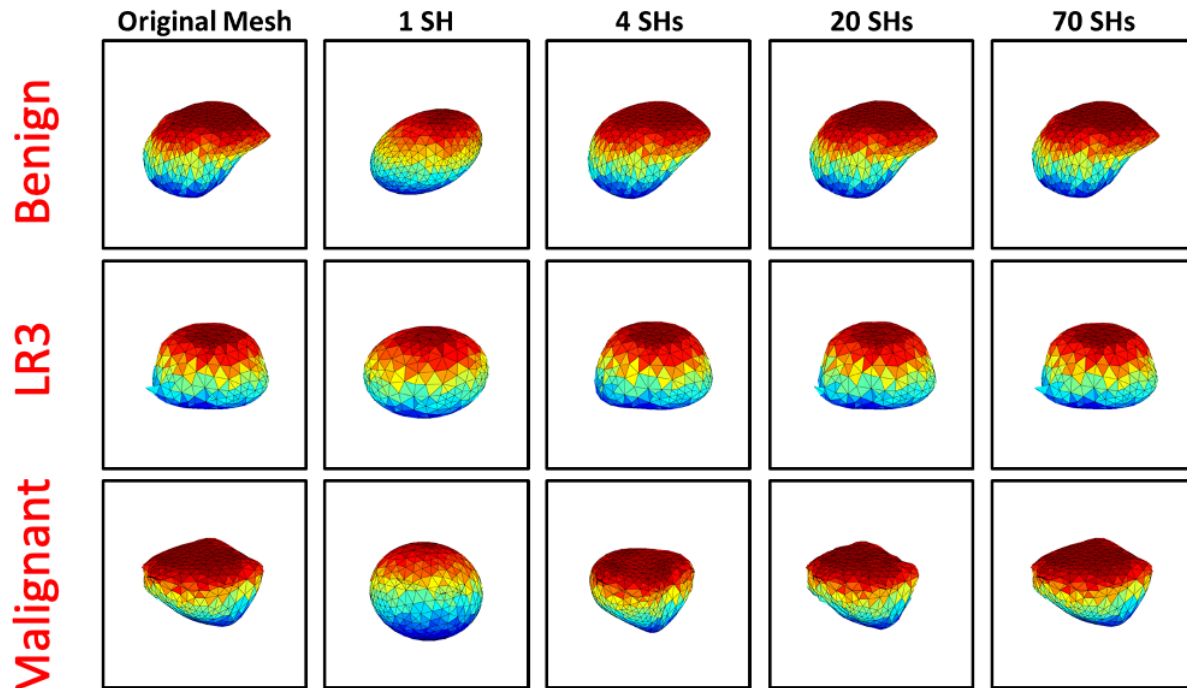
# Features Extraction: Functional Features

➤ Examine the functional hyperenhancement (wash-in) and hypo-intensity (wash-out) developed by the HCC regenerative progressive nodules.



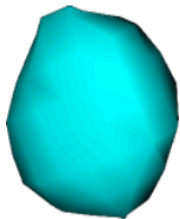
# Features Extraction: Shape Features

➤ In the proposed framework, we used the state-of-the-art spectral analysis employing spherical harmonics (SH) to extract shape features for diagnosing liver tumors.

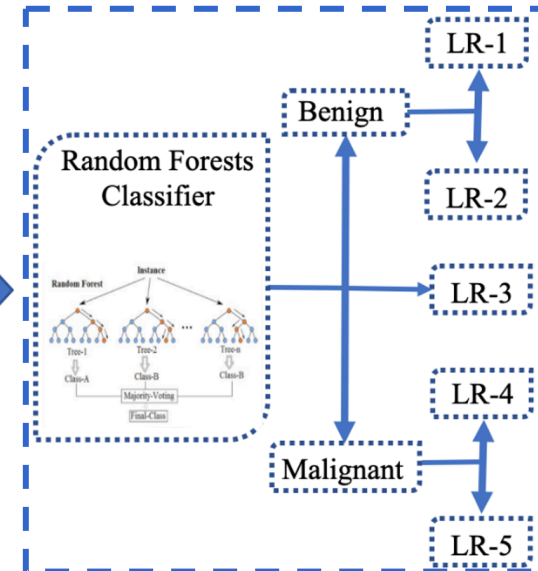


# Features Integration and Tumor Classification

- First, we started assessing the classification performance using individual features.
- Then, we integrated all the extracted features by using concatenation methods obtaining combined features and employed ML classifiers towards the final diagnosis.



Spherical Harmonics				Wash-In/Wash-Out							
70 Features/Subject				3 Features/Subject							
Shape Features				Functional Features				GLRLM Features			
								GLCM Features			
								Histogram Features			
								26 Features/Phase			
Texture Features				2 <sup>nd</sup> Order				1 <sup>st</sup> Order			
								Delayed-Contrast			
				Portal-Venous							
				Late-Arterial							
				Pre-Contrast							
				Delayed							
Pre-Contrast				Late Arterial							
Portal Venous				Pre-Contrast							
Delayed				Late Arterial							
Portal Venous				Pre-Contrast							
Delayed				Late Arterial							
Portal Venous				Pre-Contrast							
Late-Arterial				Pre-Contrast							
Pre-Contrast				Late-Arterial							
Portal-Venous				Pre-Contrast							
Delayed-Contrast				Late-Arterial							
Pre-Contrast				Late-Arterial							
Late-Arterial				Pre-Contrast							
Portal-Venous				Late-Arterial							
Pre-Contrast				Late-Arterial							
Late-Arterial				Pre-Contrast							
Pre-Contrast				Late-Arterial							
Late-Arterial				Pre-Contrast							
Pre-Contrast				Late-Arterial							
Late-Arterial				Pre-Contrast							
Pre-Contrast				Late-Arterial							
Late-Arterial				Pre-Contrast							
Pre-Contrast				Late-Arterial							
Late-Arterial				Pre-Contrast							
Pre-Contrast				Late-Arterial							
Late-Arterial				Pre-Contrast							
Pre-Contrast				Late-Arterial							
Late-Arterial				Pre-Contrast							
Pre-Contrast				Late-Arterial							
Late-Arterial				Pre-Contrast							
Pre-Contrast				Late-Arterial							
Late-Arterial				Pre-Contrast							
Pre-Contrast				Late-Arterial							
Late-Arterial				Pre-Contrast							
Pre-Contrast				Late-Arterial							
Late-Arterial				Pre-Contrast							
Pre-Contrast				Late-Arterial							
Late-Arterial				Pre-Contrast							
Pre-Contrast				Late-Arterial							
Late-Arterial				Pre-Contrast							
Pre-Contrast				Late-Arterial							
Late-Arterial				Pre-Contrast							
Pre-Contrast				Late-Arterial							
Late-Arterial				Pre-Contrast							
Pre-Contrast				Late-Arterial							
Late-Arterial				Pre-Contrast							
Pre-Contrast				Late-Arterial							
Late-Arterial				Pre-Contrast							
Pre-Contrast				Late-Arterial							
Late-Arterial				Pre-Contrast							
Pre-Contrast				Late-Arterial							
Late-Arterial				Pre-Contrast							
Pre-Contrast				Late-Arterial							
Late-Arterial				Pre-Contrast							
Pre-Contrast				Late-Arterial							
Late-Arterial				Pre-Contrast							
Pre-Contrast				Late-Arterial							
Late-Arterial				Pre-Contrast							
Pre-Contrast				Late-Arterial							
Late-Arterial				Pre-Contrast							
Pre-Contrast				Late-Arterial							
Late-Arterial				Pre-Contrast							
Pre-Contrast				Late-Arterial							
Late-Arterial				Pre-Contrast							
Pre-Contrast				Late-Arterial							
Late-Arterial				Pre-Contrast							
Pre-Contrast				Late-Arterial							
Late-Arterial				Pre-Contrast							
Pre-Contrast				Late-Arterial							
Late-Arterial				Pre-Contrast							
Pre-Contrast				Late-Arterial							
Late-Arterial				Pre-Contrast							
Pre-Contrast				Late-Arterial							
Late-Arterial				Pre-Contrast							
Pre-Contrast				Late-Arterial							
Late-Arterial				Pre-Contrast							
Pre-Contrast				Late-Arterial							
Late-Arterial				Pre-Contrast							
Pre-Contrast				Late-Arterial							
Late-Arterial				Pre-Contrast							
Pre-Contrast				Late-Arterial							
Late-Arterial				Pre-Contrast							
Pre-Contrast				Late-Arterial							
Late-Arterial				Pre-Contrast							
Pre-Contrast				Late-Arterial							
Late-Arterial				Pre-Contrast							
Pre-Contrast				Late-Arterial							
Late-Arterial				Pre-Contrast							
Pre-Contrast				Late-Arterial							
Late-Arterial				Pre-Contrast							
Pre-Contrast				Late-Arterial							
Late-Arterial				Pre-Contrast							
Pre-Contrast				Late-Arterial							
Late-Arterial				Pre-Contrast							
Pre-Contrast				Late-Arterial							
Late-Arterial				Pre-Contrast							
Pre-Contrast				Late-Arterial							
Late-Arterial				Pre-Contrast							
Pre-Contrast				Late-Arterial							
Late-Arterial				Pre-Contrast							
Pre-Contrast				Late-Arterial							
Late-Arterial				Pre-Contrast							
Pre-Contrast				Late-Arterial							
Late-Arterial				Pre-Contrast							
Pre-Contrast				Late-Arterial							
Late-Arterial				Pre-Contrast							
Pre-Contrast				Late-Arterial							
Late-Arterial				Pre-Contrast							
Pre-Contrast				Late-Arterial							
Late-Arterial				Pre-Contrast							
Pre-Contrast				Late-Arterial							
Late-Arterial				Pre-Contrast							
Pre-Contrast				Late-Arterial							
Late-Arterial				Pre-Contrast							
Pre-Contrast				Late-Arterial							
Late-Arterial				Pre-Contrast							
Pre-Contrast				Late-Arterial							
Late-Arterial				Pre-Contrast							
Pre-Contrast				Late-Arterial							
Late-Arterial				Pre-Contrast							
Pre-Contrast				Late-Arterial							
Late-Arterial				Pre-Contrast							
Pre-Contrast				Late-Arterial							
Late-Arterial				Pre-Contrast							
Pre-Contrast				Late-Arterial							
Late-Arterial				Pre-Contrast							
Pre-Contrast				Late-Arterial							
Late-Arterial				Pre-Contrast							
Pre-Contrast				Late-Arterial							
Late-Arterial				Pre-Contrast							
Pre-Contrast				Late-Arterial							
Late-Arterial				Pre-Contrast							
Pre-Contrast				Late-Arterial							
Late-Arterial				Pre-Contrast							
Pre-Contrast				Late-Arterial							
Late-Arterial				Pre-Contrast							
Pre-Contrast				Late-Arterial							
Late-Arterial				Pre-Contrast							
Pre-Contrast				Late-Arterial							
Late-Arterial				Pre-Contrast							
Pre-Contrast				Late-Arterial							
Late-Arterial				Pre-Contrast							
Pre-Contrast				Late-Arterial							
Late-Arterial				Pre-Contrast							
Pre-Contrast				Late-Arterial							
Late-Arterial				Pre-Contrast							
Pre-Contrast				Late-Arterial							
Late-Arterial				Pre-Contrast							
Pre-Contrast				Late-Arterial							
Late-Arterial				Pre-Contrast							
Pre-Contrast				Late-Arterial							
Late-Arterial				Pre-Contrast							
Pre-Contrast				Late-Arterial							
Late-Arterial				Pre-Contrast							
Pre-Contrast				Late-Arterial							
Late-Arterial				Pre-Contrast							
Pre-Contrast				Late-Arterial							
Late-Arterial				Pre-Contrast							
Pre-Contr											



# Diagnostic Results

Classifier	Approach	Accuracy	AUROC (+ve Class)			Correct Instances		
			B	LR3	M	B/34	LR3/17	M/34
RFs	LOSO	87.1%	0.95	0.92	0.91	33	11	30
	10-Fold	85.9%	0.93	0.84	0.89	31	12	30
	5-Fold	81.2%	0.88	0.89	0.87	32	9	28
KNN <sub>Fine</sub>	LOSO	85.9%	0.91	0.85	0.90	31	13	29
	10-Fold	83.5%	0.91	0.82	0.86	30	10	30
	5-Fold	78.8%	0.88	0.74	0.84	31	9	27
SVM <sub>Cub</sub>	LOSO	81.2%	0.89	0.82	0.84	30	12	27
	10-Fold	77.6%	0.85	0.73	0.87	29	9	28
	5-Fold	77.6%	0.85	0.73	0.87	29	9	28
SVM <sub>Quad</sub>	LOSO	84.7%	0.94	0.89	0.89	31	11	30
	10-Fold	82.4%	0.93	0.81	0.85	31	12	27
	5-Fold	77.6%	0.89	0.80	0.85	29	9	28

# Diagnostic Results

True Class	Predicted Class		
	Malignant	Intermediate	Benign
	Benign	33	0
Intermediate	2	11	4
Malignant	2	2	30



# Diagnostic Results

Approach	Accuracy	AUROC	Correct Instances	
LR1 vs. LR2			LR1/17	LR2/17
LOSO	91.2%	0.95	14	17
10-Fold	88.2%	0.92	13	17
5-Fold	85.3%	0.90	12	17
LR4 vs. LR5			LR4/17	LR5/17
LOSO	85.3%	0.88	16	13
10-Fold	82.4%	0.83	15	13
5-Fold	82.4%	0.83	15	13

# Summary

- The proposed HCC-CAD system has the ability to provide accurate grading for different hepatic observations according to the LI-RADS guidelines.
- Using the Random Forests classifier with a leave-one-out (LOSO) cross-validation, the developed CAD system achieved an **87.1%** accuracy in distinguishing between malignant, intermediate and benign tumors (i.e., First stage classification).
- Using the same classifier and validation, the LR-1 lesions were classified from LR-2 benign lesions with **91.2%** accuracy, while **85.3%** accuracy was achieved differentiating between LR-4 and LR-5 malignant tumors (i.e., Second stage classification).

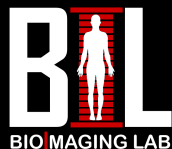
# Future work

- We have already started to collect a larger subject cohort to optimize the performance of our system in distinguishing and grading multiple hepatic observations at the same classification stage.
- Hepatic observations with LR-M will be added to our dataset to enhance the diagnostic capabilities of our CAD system.
- Automatic segmentation is being developed to reduce the computational time and subjectivity.
- Applying deep learning techniques (e.g., Autoencoder and CNN).

The University *of* Louisville

BioImaging Lab

# Thank You & Questions



Email: [ammost01@louisville.edu](mailto:ammost01@louisville.edu)

